S. Horii[1,2*], K. Takahashi[2], T. Shiozaki[3], S. Takeda[4], M. Sato[2,4], T. Yamaguchi[2,5], S. Takino[2], F. Hashihama[6], Y. Kondo[4], T. Takemura[7], and K. Furuya[8]

[1] Fisheries Resources Institute, Japan Fisheries Research and Education Agency, 1551-8, Taira-machi, Nagasaki-shi, Nagasaki, 851-2213, Japan

[2] Department of Aquatic Bioscience, Graduate School of Agricultural and Life Sciences, The University of Tokyo, 1-1-1 Yayoi, Bunkyo-ku, Tokyo, 113-8657, Japan

[3] Atmosphere and Ocean Research Institute, The University of Tokyo, 5-1-5 Kashiwanoha, Kashiwa-shi, Chiba, 277-0882, Japan

[4] Graduate School of Fisheries and Environmental Sciences, Nagasaki University, 1-14 Bunkyo-machi Nagasaki-shi, Nagasaki, 852-8521, Japan

[5] Fisheries Resources Institute, Japan Fisheries Research and Education Agency, 2-12-4 Fukuura, Yokohama-shi, Kanagawa, 236-8648, Japan

[6] Department of Ocean Sciences, Tokyo University of Marine Science and Technology, 5-7 Konan, Minato-ku, Tokyo, 108-8477, Japan

[7] Research Institute for Applied Mechanics, Kyushu University, 6-1 Kasugakouen, Kasuga-shi, Fukuoka, 816-8580, Japan

[8] Institute of Plankton Eco-engineering, Soka University, 1-236 Tangi, Hachiohji-shi, Tokyo, 192-8577, Japan

Corresponding author: Sachiko Horii (`shorii@affrc.go.jp`)

Key Points:

- Along the longitudinal transect in the subtropical North Pacific, N_2 fixation activity was high in the central area (150–180°W)
- The central North Pacific was characterized by the intermediate dust input and phosphorus stock in the euphotic zone
- East-west gradient of phosphorus availability controls the N_2 fixation in the North Pacific through co-limitation with iron

Abstract

Biological dinitrogen (N_2) fixation is an important new nitrogen source in oligotrophic subtropical oceans. In numerical model studies, the east-west gradient of iron deposition as atmospheric Asian dust strongly affects the zonal distribution of N_2 fixation activity in the North Pacific, but the in-situ relationship at a basin-scale is not well examined. We examined the trans-Pacific longitudinal variation in N_2 fixation activity from 120°W to 137°E at 23°N in summer with environmental parameters that potentially influence diazotrophy. The dissolved inorganic iron concentration in surface water was consistently low (<0.4

nM) throughout the study area. The modelled deposition flux of iron as atmospheric dust (dust-Fe) largely increased westward, whereas labile phosphorus (phosphate and labile phosphoric monoesters) in the surface water decreased westward. N_2 fixation varied between 34.6–298 µmol N m^{-2} day^{-1} and was high (>200 µmol m^{-2} day^{-1}) in the central area (150–180°W), where both dust-Fe input and the phosphorus stock were in intermediate ranges. The rates of N_2 fixation showed an increasing trend with dust-Fe input in the eastern and western parts of 180°, indicating that increasing dust input enhanced N_2 fixation activity. However, compared with that of the eastern region, the effect of enhancement on activity was smaller in the western region, where phosphate concentration in the euphotic zone was low (<50 nM), presumably due to the higher iron requirement to utilize organic phosphorus. Our data show that phosphorus availability substantially controls the longitudinal distribution of N_2 fixation through co-limitation with iron in the subtropical North Pacific.

Plain Language Summary

Biological N_2 fixation, a process that converts N_2 gas into ammonia, substantially affects biological production in subtropical ecosystems, where nitrogenous nutrients are scarce. The availability of both iron and phosphorus are primary factors that control the growth of N_2-fixing organisms. In North Pacific subtropical waters, iron input as atmospheric Asian dust is considered to control the east-west variation in N_2 fixation; however, their relationship is not well examined. Here, we examined the trans-Pacific distribution of N_2 fixation activity with environmental parameters, including iron and phosphorus availability. Our results showed that the increase in dust input enhanced N_2 fixation, but the effect on the activity was smaller in the western region (137–180°E), where phosphate was depleted in the euphotic zone, than that in the eastern region (120–180°W). This regional difference in enhancement is presumably because additional iron is required in the western region to utilize organic phosphorus. Our results indicate that phosphorus availability substantially controls the longitudinal distribution of N_2 fixation in the subtropical North Pacific through co-limitation with iron. Therefore, the dynamics of both iron and phosphorus must be considered simultaneously in terms of the utilization of organic phosphorus to predict the response of N_2 fixation to environmental changes.

1 Introduction

Biological dinitrogen (N_2) fixation, which is the process of converting N_2 gas into ammonia by specialized prokaryotes called diazotrophs, is a major new nitrogen source in the global oceans (Falkowski et al., 1998; Galloway et al., 2004). This process is particularly important for new production in oligotrophic subtropical regions. The subtropical ocean occupies 40% of the global oceans, and thus factors controlling the N_2 fixation activity are critical to understanding the global biogeochemical cycles (Karl et al., 2002).

In addition to temperature (Carpenter, 1991), the growth of diazotrophs in the subtropical ocean is largely affected by the availability of essential nutrients,

especially iron and phosphorus, as it is not limited by nitrogen availability as in the case of other marine phytoplankton (Sohm et al., 2011; Ward et al., 2013). Among these, iron input from atmospheric dust deposition is considered a primary factor controlling the basin-scale distribution of diazotrophs (Dutkiewicz et al., 2012; Moore et al., 2009; Ward et al., 2013) due to the substantial iron requirement for nitrogenase enzyme activity (Berman-Frank et al., 2001). Additionally, the availability of phosphorous, which plays an essential role in cell growth and energy supply for diazotrophs, is also important for controlling N_2 fixation (Sohm et al., 2011; Ward et al., 2013), as proven by nutrient addition experiments (Grabowski et al., 2008; Tanita et al., 2021; Watkins-Brandt et al. 2011; Wen et al., 2022).

The subtropical North Pacific has an east-west gradient of iron input from atmospheric dust deposition and phosphorous stock; atmospheric dust deposition flux from the Asian continent decreases eastward (Duce & Tindale, 1991), while both phosphate and dissolved organic phosphorus (DOP) concentrations decrease westward (Hashihama et al., 2009; 2020; Yamaguchi et al., 2021). However, N_2 fixation in the subtropical North Pacific is generally considered iron-limited rather than phosphorus-limited because of the vastness of the basin (Sohm et al., 2011; Wang et al., 2019), which restricts iron supply from the Asian continent. Therefore, prognostic biogeochemical models generally predict the westward increase in N_2 fixation at a basin-scale in the subtropical North Pacific Ocean with an increase in dust deposition (Dutkiewicz et al., 2012; Monterio et al., 2011; Wang et al., 2019). However, in situ measurements of N_2 fixation activity in the western subtropical North Pacific in previous studies (39–573 µmol N m^{-2} d^{-1}; Shiozaki et al., 2009, 2010; Tanita et al., 2021; Wen et al., 2022) are not necessarily higher than those in the central and eastern regions, which show rates between 87 and 520 µmol N m^{-2} d^{-1} (Montoya et al., 2004; Wilson et al., 2008; Böttjer et al., 2017; Shiozaki et al., 2017). This inconsistency suggests that iron input through atmospheric dust deposition is not the single factor controlling the geographic variation of N_2 fixation activity in the subtropical North Pacific, although no adequate observation to examine this has been made to date.

Here, we conducted a trans-Pacific observation at 23°N from 120°W to 137°E in summer (August–September) to examine the east-west variations in N_2 fixation in relation to iron and phosphorus availability. As a proxy for iron supply, the iron flux from atmospheric dust deposition (dust-Fe) was simulated during cruise periods, and the concentrations of dissolved inorganic iron (DFe) were determined by onboard observations. We examined the concentrations of phosphoric monoesters, major labile organic phosphorus, and phosphate using a highly sensitive analytical method. Additionally, the abundance of *nifH* genes of major diazotrophs was determined to examine their relationship with the geographical variation in N_2 fixation activity. This study shows the importance of phosphorus as a controlling factor affecting the distribution of N_2 fixation in the subtropical North Pacific Ocean, as well as iron, through dust deposition flux.

2 Materials and Methods

2.1 Study site, physical and chemical parameters, and chlorophyll *a*

This study was conducted at 12 stations from 21 August to 1 October 2017, along the meridional transect from 120°W to 137°E on the 23°N line in the North Pacific subtropical region by the KH-17-4 cruise onboard the R/V *Hakuho-maru* (Figure 1 and Table 1). Temperature and salinity profiles were obtained using a conductivity, temperature, and depth (CTD) system (Sea-Bird Electronics, Inc., Washington, D. C., USA), and light intensity was measured using a Hyper Profiler (Satlantic LP, Halifax, NS, Canada). Euphotic zone depth was defined as 1% light depth.

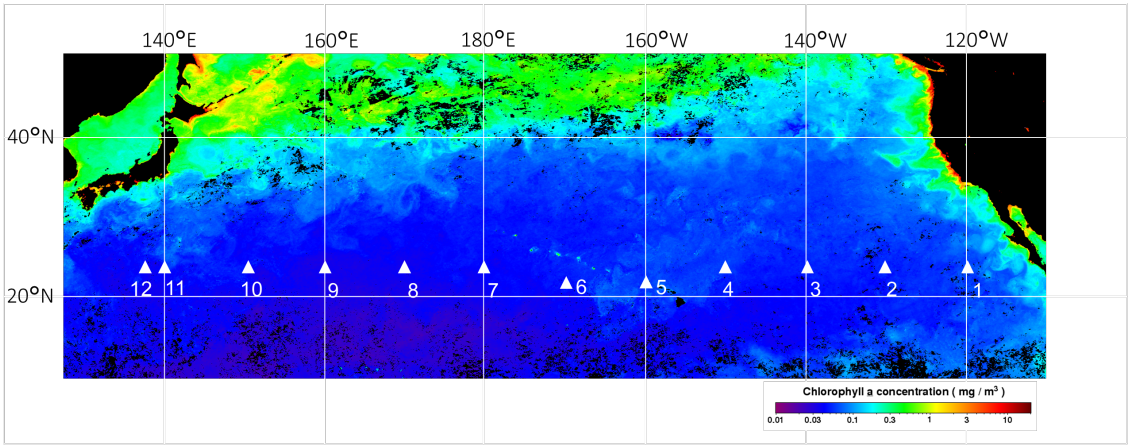

Figure 1. Stations where samplings and observations were performed from August 21st to October 1st in 2017 during the KH-17-4 cruise. Chlorophyll *a* concentration derived from MODIS-Aqua (https://oceancolor.gsfc.nasa.gov/l 3/) in September 2017 is also shown.

All water samples were collected using an acid-cleaned bucket or Teflon-coated 12-L Niskin-X bottles on a CTD-Carousel system connected to a Vectran cable between the surface and a depth of 200 m. The water samples for the macronutrients and chlorophyll *a* (chl *a*) were directly collected from Niskin-X bottles or buckets into plastic bottles. The concentrations of nitrate and phosphate were determined onboard using a super-sensitive colorimetric system (Hashihama et al., 2009). The detection limits of both nitrate and phosphate were 3.0 nM. When the concentration was higher than 1 µM, the samples were frozen, and the concentrations were determined using an AACSII auto-analyzer on land (Bran+Luebbe, Hamburg, Germany). The concentration of labile phosphoric monoesters was measured using the enzymatic hydrolysis method described by Yamaguchi et al. (2021), and the detection limit was 3.4 nM. For chl *a*, an aliquot of 260 mL water was gently filtered using 25-mm Whatman GF/F filters, and the concentration was fluorometrically measured using a 10-AU fluorometer (Turner Designs, CA, USA) after extraction with *N, N*-dimethylformamide

(Suzuki & Ishimaru, 1990; Welschmeyer, 1994).

Table 1. The information of the samplings and environmental variables at each station in the KH-17-4 cruise.

Station	Date (GMT)	Latitude	Longitude	% light depth [m]	SST [°C]	Dust-Fe [nmol m^{-2} day^{-1}]	DFe (µmol m^{-2})	Phosphate (mmol m^{-2})	Phosphomonoesters (mmol m^{-2})	N_2 fixation activity [mol N m^{-2} d^{-1}]	Primary production [mmol C m^{-2} day^{-1}]	N_2 fix/PP ratio (%)
	/8/21	° 00’ N	° 00’ W									
	/8/25	° 00’ N	° 00’ W									
	/8/28	° 00’ N	° 00’ W									
	/8/31	° 00’ N	° 00’ W									
	/9/3	° 30’ N	° 00’ W									
	/9/14	° 30’ N	° 00’ W									
	/9/17	° 00’ N	° 00’ W									
	/9/20	° 00’ N	° 00’ E									
	/9/23	° 00’ N	° 00’ E									
	/9/27	° 00’ N	° 00’ E									

Station	Date (GMT)	Latitude	Longitude	1% light depth [m]	SST [°C]	Dust-Fe [nmol m^{-2} day^{-1}]	DFe (µmol m^{-2})	Phosphate (mmol m^{-2})	Labile phosphoric monoesters (mmol m^{-2})	N_2 fixation activity [mol N m^{-2} d^{-1}]	Primary production [mmol C m^{-2} day^{-1}]	N_2 fix/PP ratio (%)
	/9/30	° 00' N	° 00' E									
	/10/1	° 00' N	° 00 E									

Notes: SST indicates sea surface temperature. Dust-Fe indicates 14-days average of daily iron input as atmospheric dust deposition modelled by SPRINT-ARS before the observation. The integrated amounts of dissolved inorganic iron (DFe), phosphate and labile phosphoric monoesters in the euphotic zone were shown. The euphotic zone depth was defined as the depth of 1% light depth, but it was substituted by the depth of subsurface chlorophyll maximum (102–140 m) for DFe amount. The integrated rates in the water column were shown for N_2 fixation activity. N_2 fix/PP ratio indicates N2 fixation activity × 6.6/primary production × 100, 6.6 is the Redfield ratio.

Samples for dissolved inorganic iron (DFe) concentration were taken from Niskin-X bottles, which were placed in a clean air booth immediately after recovery. Seawater was typically taken from depths of 10, 20, 50, 100, 150, and 200 m and subsurface chl *a* maximum (SCM), and filtered through an AcroPak 200 Capsule filter unit having 0.2 m pore-size Supor Membrane (Pall Co., NY, USA) attached directly to the spigot with silicon tubing under pressure by compressed clean air. Filtered seawater samples were collected in acid-cleaned 125-ml low-density polyethylene (LDPE) bottles and acidified to pH <1.7 with 20% quartz-distilled HCl (TAMAPURE AA-100, Tama Chemicals Co., Kanagawa, Japan). The acidified water samples were stored at room temperature for more than one year before analysis. The concentration of DFe was determined by cathodic stripping voltammetry after complexation of 2,3-dihydroxynaphthalene (DHN) with ferric ions and the standard addition method, as described by Obata and van den Berg (2001). The detection limit of the DFe was 0.03 nM

2.2 N_2 fixation activity and primary production

N_2 fixation activity and primary production were measured according to the

^{15}N-^{13}C dual inlet technique (Shiozaki et al., 2017), which combined the $^{15}N_2$ gas dissolution method (Mohr et al., 2010) with a ^{13}C primary production assay (Hama et al., 1983), for the six depths corresponding to incident light levels of 100%, 25%, 10%, 1%, and 0.1%, and at a depth of 10 m. Water samples for incubation were collected in duplicate acid-cleaned 4.5 L PC bottles covered by neutral-density screens to adjust the light levels with initial samples, which were immediately filtered onto pre-combusted GF/F filters. $^{15}N_2$-enriched seawater prepared using a Sterapore membrane unit (20M1500A; Mitsubishi Rayon Co., Ltd., Tokyo, Japan) and ^{13}C-labeled sodium bicarbonate (99% atom% ^{13}C; Cambridge Isotope Laboratories, Inc., MA, USA) were added to the seawater for incubation. Seawater was incubated on the deck in a running seawater bath for 24 h and then filtered onto pre-combusted GF/F filters. All filter samples were kept at −20°C until later measurements on land. For the measurement, the filter samples were oven-dried at 50°C, exposed to HCl fumes for 2 h to remove the carbonate, and dried again at 50°C. The nitrogen and carbon contents and their stable isotopic ratios were determined using a DELTA V Advantage mass spectrometer (Thermo Electron, MA, USA) connected to an elemental analyzer. The rates of N_2 fixation and primary production were calculated according to Montoya et al. (1996) and Hama et al. (1983), respectively. We considered N_2 fixation activity to be significant when the proportion of ^{15}N in the nitrogen content for each incubated bottle was higher than that of the initial sample by 0.00146 atom % (Montoya et al., 1996).

2.3 DNA analyses for diazotrophs community

Water samples for qPCR analyses of *nifH* genes of major diazotrophs were collected in 1.1 L polypropylene bottles from the same Niskin bottles concurrently with the sampling for determining N_2 fixation activity and were filtered onto 0.2 m Nuclepore filters (Whatman plc., Kent, UK). All filter samples were kept frozen at -−20°C until analysis. DNA was extracted using a ChargeSwitch Forensic DNA Purification Kit (Invitrogen, Carlsbad, CA, USA), following the manufacturer's instructions. We quantified six groups of diazotrophs, which are known to be major in the North Pacific subtropical water (Shiozaki et al., 2017); heterotrophic -proteobacterium -24774A11, symbiotic cyanobacteria UCYN-A1 associated with haptophytes, *Richelia intracellularis* associated with diatoms belonging to *Rhizosolenia clevei* (RR), *R. intracellularis* associated with diatoms belonging to *Hemiaulus hauckii* (RH), filamentous cyanobacteria *Trichodesmium* spp., and unicellular cyanobacterium *Crocosphaera watsonii*. The sets of primers, probes, and standards are described in Supporting Information Table S1. We conducted a qPCR assay using the Mini Opticon Real-Time PCR System (BIO-RAD, CA, USA). The 20 l reactions contain10 l 2×PreMix Ex Taq (Probe qPCR, Takara Bio Inc., Shiga, Japan), 6.4 l Milli-Q water, 2 l template DNA, 0.6 l for each of the10 M forward and reverse primers, and 0.4 l for 10 M Taqman probe. At least triplicate PCR amplifications were performed for each sample with the following parameters: 95°C for 5 min, followed by 49 cycles of 95°C for 4 s and 60°C for 11 s. Standards consisting of six 10-fold dilutions of *nifH* gene fragments (10^6–10^1 copies) and a negative control were

prepared for each plate. The copy numbers of the target genes in the DNA samples were calculated from the mean Ct value for each sample. The r^2 values of the standard curves were always >0.99, and no signal was detected in the negative controls. PCR efficiencies were between 89.0% and 111.1%, and the detection limit was 75 copies L^{-1}.

2.4 Atmospheric dust deposition

Daily dry and wet deposition of soil dust was calculated using a three-dimensional aerosol climate model SPRINTARS version 6.1.0 at 1.12°×1.12° resolution, which was developed using the framework of an atmospheric general circulation model MIROC (Takemura et al., 2000, 2002, 2005). We assumed that the iron content of dust was 3.5% (Duce & Tindale 1991) and calculated the daily flux of iron as atmospheric dust (dust-Fe) at each station. The 14-days average of daily deposition before the date of observation was used for the analyses, according to Hashihama et al. (2009).

3 Results

3.1 Environmental conditions

Sea surface temperature (SST) and sea surface salinity tended to increase westward from 24°C to 30°C and from 34.4 to 35.2, respectively, along the transect (Figures 2a, b). The euphotic zone depth varied in the range of 104–117 m and did not show notable longitudinal variation (Table1, Figure 2). The concentration of chl *a* did not show an apparent east-west variation, and subsurface chlorophyll *a* maximum (SCM) was always observed around the 1% light depth (Figure 2c). Nitrate was mostly depleted (<10 nM) in the euphotic zone (Figure 2d) and there was no clear longitudinal gradient. Phosphate and labile phosphoric monoesters in the euphotic zone decreased westward from >200 nM to <10 nM and from >30 nM to <10 nM, respectively (Figures 2e and f). The depth-integrated amount of phosphate and phosphoric monoesters in the euphotic zone decreased westward from 25 to <2.5 mmol m^{-2} with an increasing proportion of phosphoric monoesters (Figure 3a, Table 1). Either the DFe concentration at a depth of 10 m (0.11–0.40 nM, data not shown) or the integrated amount in the euphotic zone (11–56 mol m^{-2}) had no significant east-west difference (Figure 3b, Table 1). Contrastingly, the dust-Fe flux generally increased westward (Figure 3b, Table 1), and its mean value in the area west of 180° (423±184 nmol Fe m^{-2} day^{-1}; St. 7–12) was significantly higher than that in the area east of 180° (154±74.4 nmol Fe m^{-2} day^{-1}; St. 1–6) (p <0.05, t-test).

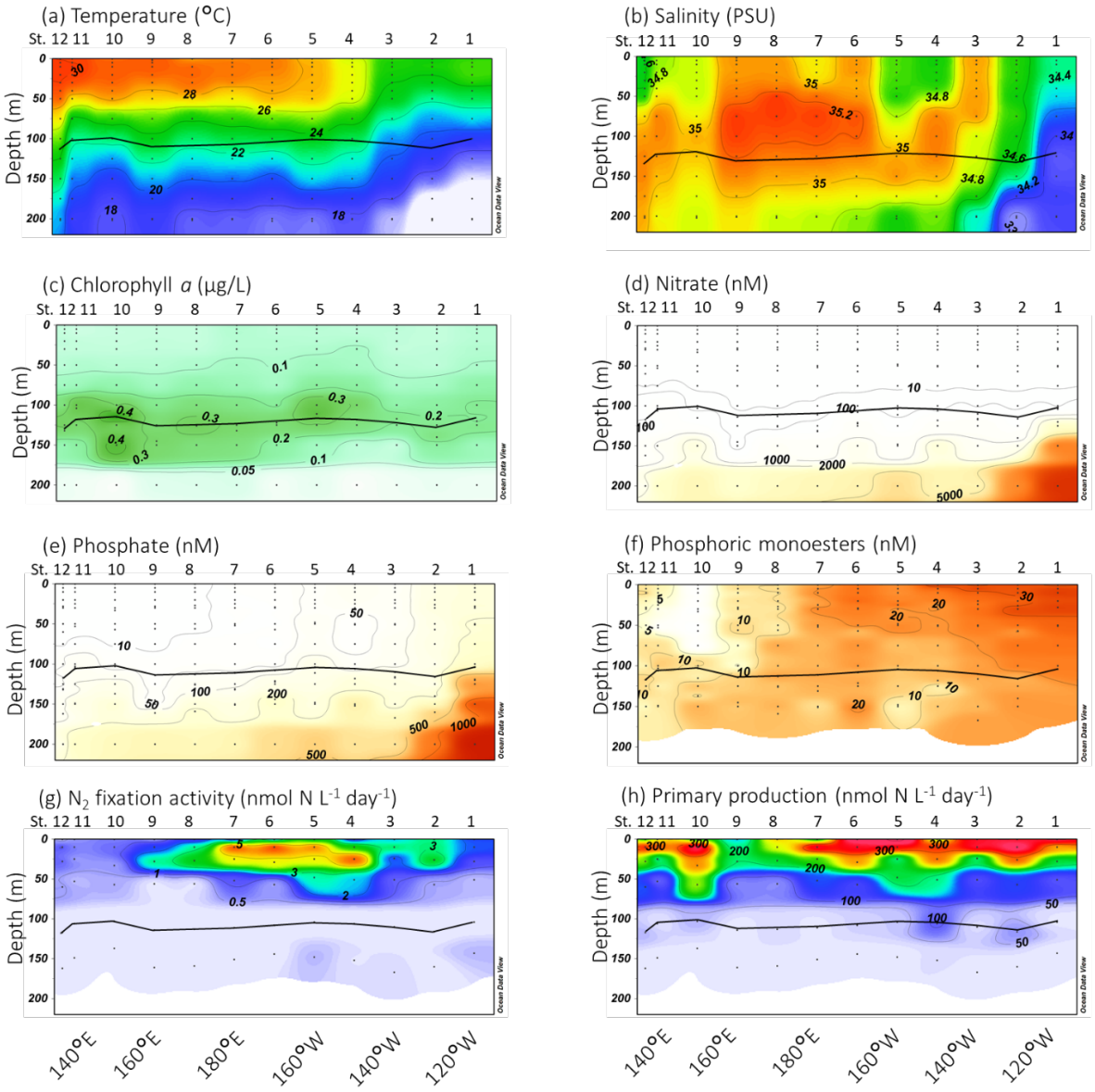

Figure 2. Profiles of the environmental variables at the stations along the cruise track during the KH-17-4 cruise. Vertical profiles of (a) temperature, (b) salinity, concentrations of (c) chlorophyll *a*, (d) nitrate, (e) phosphate, (f) labile phosphoric monoesters, (g) N_2 fixation activity and (h) primary production. Black bold line indicates the 1% light depth.

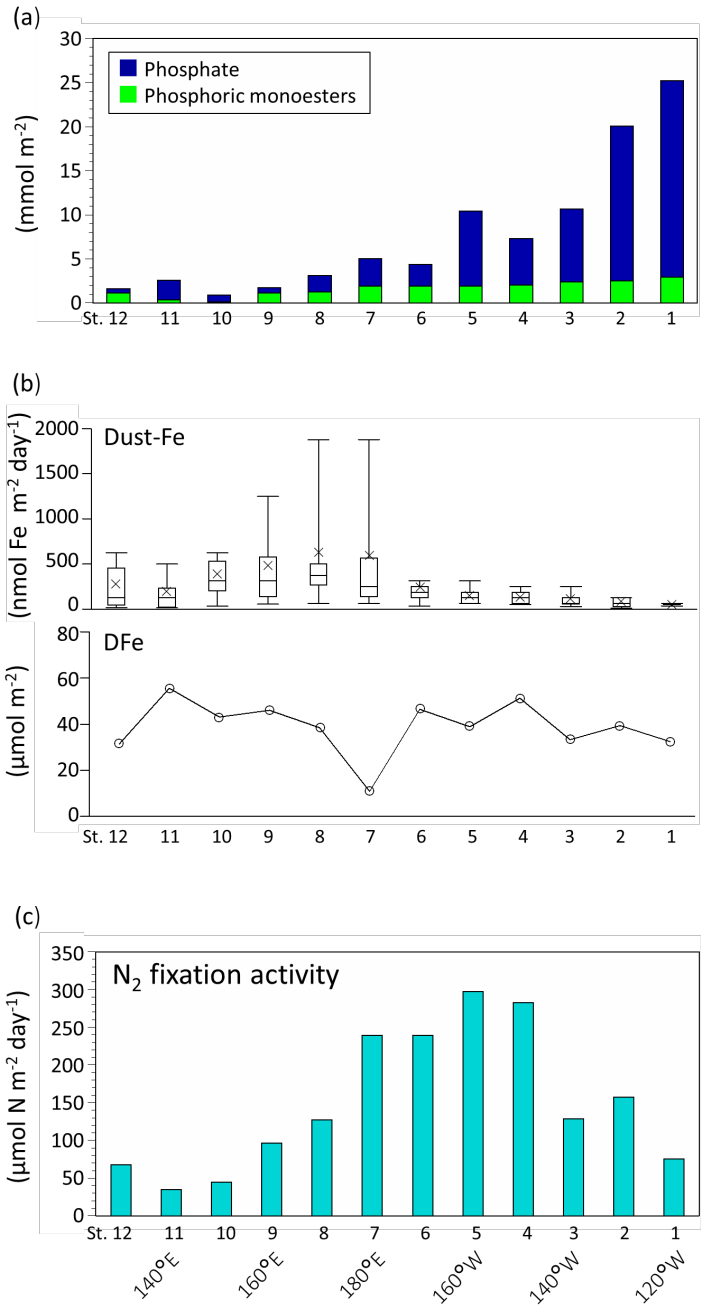

Figure 3. Longitudinal variations in N_2 fixation activity, phosphorus and iron conditions along the cruise track during the KH-17-4. (a) The integrated amounts of phosphate and labile phosphoric monoesters in the euphotic zone.

(b) The calculated daily flux of iron deposition as atmospheric dust (dust-Fe), which was modelled by SPRINTARS for 14 days before the observation, and the integrated amount of dissolved inorganic iron (DFe) in the euphotic zone. (c) The integrated rates of N_2 fixation activity in the water column. Crosses and solid lines in the box plot indicate averages and medians, respectively.

3.2 N_2 fixation activity and primary production

The rates of N_2 fixation activity and primary production were high in the upper layer, from the surface to a depth of 20–30 m, which corresponded to the upper layer at 25% light depth (Figures 2g and f). The maximum and depth-integrated N_2 fixation in the water column varied between 0.5–7.1 nmol N L^{-1} day^{-1} and 34.6–298 µmol N m^{-2} day^{-1}, respectively, and increased in the central region from St. 4 to 7 (Figures 2g and 3c, Table 1). Although no significant correlation was found between integrated N_2 fixation and any of the environmental variables throughout the transect ($p > 0.05$, Figure 4, Supporting Information Figure S1), both iron and phosphorus showed significant correlations ($p < 0.05$) with N_2 fixation depending on the longitudinal range: east (St. 1–6) and west (St. 7–12) of 180°. In the western region, N_2 fixation activity was significantly and positively correlated with dust-Fe flux and negatively correlated with DFe flux ($p < 0.05$, Figures 4c and d). For phosphorus, N_2 fixation showed significant positive and negative correlations with phosphoric monoesters in the western and eastern regions, respectively ($p < 0.05$, Figures 4a, b).

Compared with N_2 fixation, the longitudinal variation in the depth-integrated primary production was relatively small, which ranged between 11.7–25.1 mmol C m^{-2} day^{-1} (Table 1, Supporting Information Figure S2a). Generally, the primary production was positively correlated with depth-integrated N_2 fixation, except at the western end of the transect from St. 10 to 12 ($p < 0.05$, Supporting Information Figure S2b). The calculated contribution of the fixed nitrogen to primary production at the stations at the western end of the transect (St. 10–12) was consistently lower than that at the other stations (1.2–2.1% v.s. 3.5–9.9%; Supporting Information Figure S2a).

3.3 Distributions of major diazotrophs

The *nifH* genes detected in this study were mainly composed of three cyanobacteria, *Crocosphaera watsonii*, *Trichodesmium* spp., and UCYN-A1, whose depth-integrated abundances were more than ten times higher than those of the other diazotrophs, -24774A11, and two types of *Richelia intracellularis* (Figure 5 and Supporting Information S3). The total abundance of the diazotrophs was especially high at St. 4 and 5, corresponding to the stations where active high N_2 fixation was found (Figure 5). *C. watsonii* and *Trichodesmium* spp. were widely distributed at stations between St. 4 and St. 12, whereas they rarely occurred at St. 1–3 (Figure 5, Supporting Information Figures S3a and b). Contrastingly,

UCYN-A1 dominated the community at the eastern stations from St. 1 to 3 (Figure 5, Supporting Information Figure S3c).

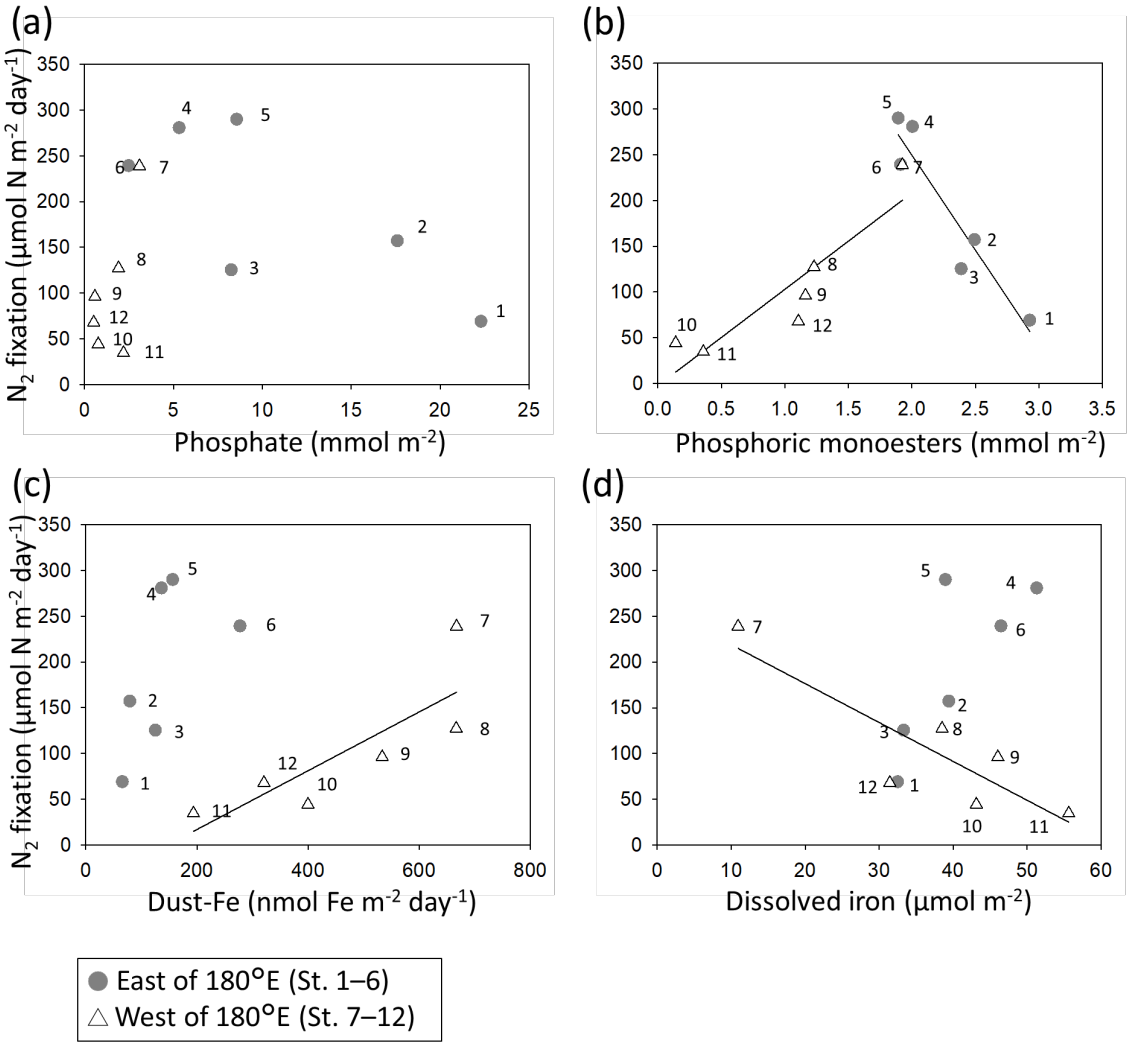

Figure 4. Relationships between N_2 fixation activity in the water column and the environmental variables during the KH-17-4 cruise. The relationship with the integrated amount in the euphotic zone of (a) phosphate, (b) labile phosphoric monoesters, (d) dissolved iron and (c) the calculated 14-days average of the daily flux of iron deposition as atmospheric dust (dust-Fe) before the observation, which was modelled by SPRINTARS. Station numbers are shown beside the plots. Regression lines are shown when the relationships were significant (p <0.05).

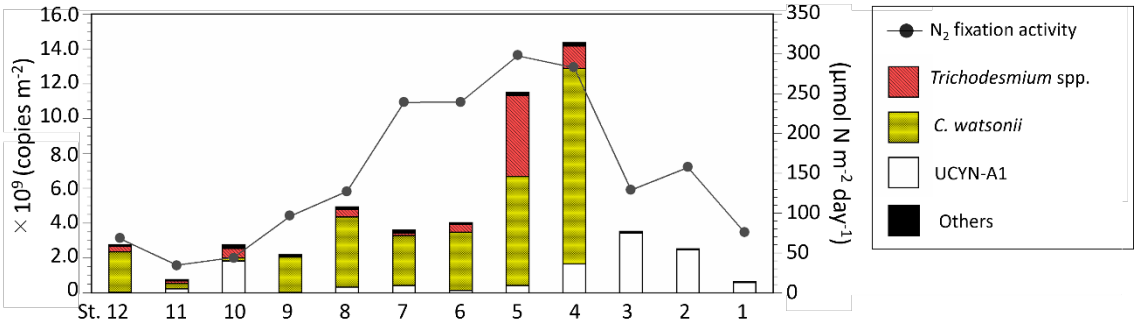

Figure 5. The longitudinal variations in depth-integrated abundances of *nifH* gene abundances for the diazotrophs quantified by qPCR analyses and N_2 fixation activity during the KH-17-4.

4 Discussion

4.1 Factors determining the longitudinal distribution of N_2 fixation in this study

The trans-Pacific observation along the 23°N transect revealed that the N_2 fixation activity was particularly high (238–283 µmol N m^{-2} day^{-1}) in the central area from 180° to 150°W, and decreased both eastward and westward (34.6–157 µmol N m^{-2} day^{-1}). This is different from the pattern simulated by numerical models, which increased westward, reflecting the westward increase in the Asian dust input (Dutkiewicz et al., 2012; Monterio et al., 2010). Therefore, our results suggest that the basin-scale distribution of N_2 fixation activity in the subtropical North Pacific is substantially controlled not only by dust Fe input but also by other factors.

In this study, the DFe concentration at a depth of 10 m was substantially low (0.11–0.40 nM) and within the range of those when iron limitation on diazotrophs occurred in subtropical open waters (Cerdan-Garcia et al., 2022; Tanita et al., 2021), indicating that bio-available iron was scarce throughout the study area. Therefore, iron input, rather than stock, is a more appropriate parameter to examine the relationship between iron availability and N_2 fixation. The N_2 fixation activity showed increasing trends with the dust-Fe input, although the degree of the response against the input was different between the eastern and western areas of 180° (Fig. 4c). In short, the N_2 fixation activity was positively correlated with the dust-Fe input in the western area of 180° (Fig. 4c), while a similar level of the activity was also observed in the eastern area, where the dust-Fe input was consistently lower than that in the western area. This indicates that the diazotroph community in the eastern area (St. 1–6) could perform up to 10 times higher N_2 fixation activity than that in the western area (St. 7–12) under a similar range of dust-Fe input. As the diazotroph communities at the

stations with relatively high N_2 fixation activity in both areas (St. 4–6 vs. St. 7–9) were similarly dominated by *Crocosphaera watsonii* and *Trichodesmium* spp., it is more likely that the diazotroph community in each area was under different physiological conditions in terms of its response to dust-Fe input.

We found that phosphate was depleted in the western region; the concentration in the euphotic zone (<50 nM) corresponded to the level that could limit N_2 fixation activity in the North Pacific (Letelier et al., 2019; Tanita et al., 2020; Wen et al., 2022). In the western area, N_2 fixation activity was positively correlated with the concentration of labile phosphoric monoesters (Figure 4b), which is known as an alternative source of phosphorous for cyanobacterial diazotrophs when phosphate is deficient (Yamaguchi et al. 2019, 2021). This relationship suggests that N_2 fixation in the western area is also limited by phosphorus.

The co-limitation of iron and phosphorus on N_2 fixation activity was reported in the phosphate-depleted waters of the Atlantic Ocean (Mills et al., 2004) and was recently proved through nutrient enrichment experiments in the western North Pacific Ocean (Tanita et al., 2021; Wen et al., 2022). Therefore, the results of this study are supported by an experimental approach. During the same cruise, high rates of phosphoric monoesterase activity were observed in the western area (Yamaguchi et al., 2021). Dissolved organic phosphorus (DOP) is generally considered an important phosphorus source for diazotrophs in phosphate-depleted waters (Cerdan-Garcia et al., 2022; Watkins-Brandt et al., 2011). However, the utilization of DOP in the field is often limited by iron availability because PhoX, the most widely distributed type of phosphatase among marine microbes, including diazotrophs, requires iron as a metal cofactor (Browning et al., 2017; Liang et al., 2022; Rouco et al., 2018). Such iron limitation on DOP utilization could also be severe when labile phosphoric monoesters are depleted (<10 nM), given that bulk DOP consistently remains >100 nM in the western area (Yamaguchi et al., 2021) and PhoX can hydrolyze a wide range of DOP substrates (Zaheer et al., 2009). Consequently, the microbes, including diazotrophs, in the phosphate-depleted western area are considered to require more iron-enriched conditions to attain phosphorous, resulting in iron and phosphorus co-limitation on N_2 fixation, despite a relatively enriched supply of dust-Fe. The co-limitation is expected to relax eastward with increasing phosphate concentration in the euphotic zone, while iron limitation in the eastern area will relax westward with increasing dust-Fe input, resulting in the observed N_2 fixation pattern in this study with a prominent peak between 150–180°W.

4.2 Possible spatiotemporal variation in N_2 fixation in the subtropical North Pacific

The widespread depletion of phosphate in the euphotic zone was reported in the western part of the subtropical North Pacific, which was largely attributed to the active N_2 fixation enhanced by the abundant dust-Fe input from the

Asian continent (Deutsch et al., 2001; Hashihama et al., 2009; Martiny et al., 2019). Therefore, the iron and phosphorus co-limitation suggested in this study is generally applicable for N_2 fixation in this region. Since microbes, including diazotrophs, require additional iron to utilize DOP under phosphate-depleted conditions, the level of dust-Fe input will ultimately determine N_2 fixation in the subtropical western North Pacific. For example, during spring, when Asian dust input generally becomes the highest within the year (Zhu et al., 2007), the rates of N_2 fixation in the western North Pacific could be as high as 500–600 μmol N m^{-2} day^{-1} (Wen et al., 2022). A similar level of enhancement was also reported in phosphate-depleted waters (<10 nM) in the tropical North Atlantic Ocean, in which dust-Fe input is approximately 10 times higher than that in the North Pacific (Luo et al., 2014; Tang et al., 2019). Therefore, the geographic pattern predicted in the prognostic biogeochemical models, in which N_2 fixation activity increases westward (Dutkiewicz et al., 2012; Monterio et al., 2010), will be observed only when dust-Fe input is abundant. Collectively, although the results of this study are a snapshot of summer, the geographic variation in N_2 fixation with its peak in the central area possibly reflected the annually averaged pattern of N_2 fixation in the subtropical North Pacific, which is similar to that of a pattern proposed for the long-term trend of N_2 fixation based on inverse models using basin-scale phosphorus and nitrogen distributions (Wang et al., 2019).

The geographic pattern in the N_2 fixation found in this study is also compatible with the possible effect of islands: the frequent occurrences of hotspots of diazotrophs near the islands, which were reported near the Hawaiian Islands as well as the western South Pacific (Bonnet et al., 2018; Dutheil et al., 2018; Shiozaki et al., 2014c). This phenomenon can be explained by the relatively enriched supply of either iron or phosphate from the deep layer (Itoh et al., 2021), or from the sedimentary sources around the islands (Dutheil et al., 2018), because the N_2 fixation activity near the Hawaiian Islands could be limited by either iron or phosphorus (Grabowski et al., 2008), although the activity was considered iron-limited in the eastern area in this study.

5 Conclusions

This study is the first field observation that shows the importance of phosphate, as well as iron, in controlling the east-west gradient of N_2 fixation activity in the subtropical North Pacific, where phosphate concentration decreases westward while dust-Fe input from the Asian continent decreases eastward. Despite the enriched dust-Fe input, N_2 fixation was relatively low in the western area of 180°, where phosphate was depleted, suggesting iron and phosphorus co-limitation. Contrastingly, the iron supply largely controlled N_2 fixation in the eastern area of 180°, where phosphate was replenished. Consequently, N_2 fixation activity peaked in the central area (150–180°W), where both dust-Fe input and phosphorus stocks were in intermediate ranges within the transect.

It is anticipated that the vertical supply of phosphate to the euphotic zone will be weakened by global warming due to the strengthening of ocean stratification

(Sallée et al. 2021). Therefore, phosphorus limitation on N_2 fixation in the North Pacific will be more serious, especially in the western area, where phosphate deficiency is widespread (Hashihama et al., 2009; Martiny et al., 2019). Simultaneously, more iron will be required to sustain N_2 fixation in the future because iron availability limits the utilization of DOP, which is an alternative phosphorus source for microbes, including diazotrophs. Therefore, the dynamics of both iron and phosphorus need to be considered simultaneously in future studies to predict the response of ecosystems and biogeochemical cycles to environmental changes, particularly in the subtropical Pacific, where N_2 fixation is an essential nitrogen source controlling primary production.

Acknowledgments

We would like to thank the crew members of R/V *Hakuho-maru* for their assistance in the observations and sample collection. Thanks to Mr. Y. Fujita for the collection of dissolved trace metal samples. This work was supported by MEXT/JSPS KAKENHI Grant Numbers JP24121005, JP24121001, JP16H04959, JP16J06708, JP16J08143, JP16K12586, JP19H05669, JP20KK0240, JP21H03592, JP24121003 and a research grant from Asahi Group Foundation.

Data Availability Statement

Data used in this article are available through UTokyo repository (http://hdl.handle.net/2261/0002005662). Spectral Radiation-Transport Model for Aerosol Species SPRINTARS is available in https://sprintars.riam.kyushu-u.ac.jp/indexe.html. We showed the range of the concentration of dissolved inorganic iron and its integrated abundance in the euphotic zone in the manuscript, which were the parameters directly used in this study, but the original data of the concentration was not shown because it is planned to be shown in another paper under preparation.

References

Berman-Frank, I., J. T. Cullen, Y. Shaked, R. M. Sherrell, and P. G. Falkowski (2001), Iron availability, cellular iron quotas, and nitrogen fixation in *Trichodesmium*, *Limnology and Oceanography*, *46*(6), 1249-1260.

Bonnet, S., M. Caffin, H. Berthelot, O. Grosso, M. Benavides, S. Helias-Nunige, C. Guieu, M. Stenegren, and R. A. Foster (2018), In-depth characterisation of diazotroph activity across the western tropical South Pacific hotspot of N_2 fixation (OUTPACE cruise), *Biogeosciences*, *15*(13), 4215-4232, doi:10.5194/bg-15-4215-2018.

Böttjer, D., J. E. Dore, D. M. Karl, R. M. Letelier, C. Mahaffey, S. T. Wilson, J. Zehr, and M. J. Church (2017), Temporal variability of nitrogen fixation and particulate nitrogen export at Station ALOHA, *Limnology and Oceanography*, *62*(1), 200-216, doi:10.1002/lno.10386.

Browning, T. J., E. P. Achterberg, J. C. Yong, I. Rapp, C. Utermann, A. Engel, and C. M. Moore (2017), Iron limitation of microbial phosphorus

acquisition in the tropical North Atlantic, *Nature Communication*, *8*, 15465, doi:10.1038/ncomms15465.

Carpenter, E. J., and K. Romans (1991), Major role of the cyanobacterium *Trichodesmium* in nutrient cycling in the North Atlantic Ocean, *Science*, *254*, 1356-1358.

Cerdan-Garcia, E., A. Baylay, D. Polyviou, E. M. S. Woodward, L. Wrightson, C. Mahaffey, M. C. Lohan, C. M. Moore, T. S. Bibby, and J. C. Robidart (2022), Transcriptional responses of *Trichodesmium* to natural inverse gradients of Fe and P availability, *ISME J*, *16*(4), 1055-1064, doi:10.1038/s41396-021-01151-1.

Deutsch, C., N. Gruber, R. M. Key, J. L. Sarmiento, and A. Ganachaud (2001), Denitrification and N_2 fixation in the Pacific Ocean, *Global Biogeochemical Cycles*, *15*(2), 483-506, doi:10.1029/2000gb001291.

Duce, R. A., and N. W. Tindale (1991), Atmospheric transport of iron and its deposition in the ocean, *Limnology and Oceanography*, *36*, 1715-1726.

Dutheil, C., O. Aumont, T. Gorguès, A. Lorrain, S. Bonnet, M. Rodier, C. Dupouy, T. Shiozaki, and C. Menkes (2018), Modelling N_2 fixation related to *Trichodesmium* sp.: driving processes and impacts on primary production in the tropical Pacific Ocean, *Biogeosciences*, *15*(14), 4333-4352, doi:10.5194/bg-15-4333-2018.

Dutkiewicz, S., B. A. Ward, F. Monteiro, and M. J. Follows (2012), Interconnection of nitrogen fixers and iron in the Pacific Ocean: Theory and numerical simulations, *Global Biogeochemical Cycles*, *26*(1), GB1012, doi:10.1029/2011gb004039.

Falkowski, P. G., B. T. Barber, and V. Smeacek (1998), Biogeochemical controls and feedbacks on ocean primary production, *Science*, *281*(5374), 200-206.

Foster, R. A., A. Subramaniam, C. Mahaffey, E. J. Carpenter, D. G. Capone, and J. P. Zehr (2007), Influence of the Amazon River plume on distributions of free-living and symbiotic cyanobacteria in the western tropical north Atlantic Ocean, *Limnology and Oceanography*, *52*(2), 517-532, doi:10.4319/lo.2007.52.2.0517.

Galloway, J. N., et al. (2004), Nitrogen Cycles: Past, Present and Future, *Biogeochemistry*, *70*, 153–226, doi:10.1007/s10533-004-0370-0.

Grabowski, M. N. W., M. J. Church, and D. M. Karl (2008), Nitrogen fixation rates and controls at Stn ALOHA, *Aquatic Microbial Ecology*, *52*, 175-183, doi:10.3354/ame01209.

Hama, T., T. Miyazaki, Y. Ogawa, T. Iwakuma, M. Takahashi, A. Otsuki, and S. Ichimura (1983), Measurement of photosynthetic production of a marine phytoplankton population using astable ^{13}C isotope, *Marine Biology*, *73*, 31-36.

Hashihama, F., K. Furuya, S. Kitajima, S. Takeda, T. Takemura, and J. Kanda (2009), Macro-scale exhaustion of surface phosphate by dinitrogen fixation

in the western North Pacific, *Geophysical Research Letters*, *36*(3), n/a-n/a, doi:10.1029/2008gl036866.

Hashihama, F., et al. (2020), Biogeochemical controls of particulate phosphorus distribution across the oligotrophic subtropical Pacific Ocean, *Global Biogeochemical Cycles*, *34*(9), doi:10.1029/2020gb006669.

Itoh, S., H. Kaneko, S. Kouketsu, T. Okunishi, E. Tsutsumi, H. Ogawa, and I. Yasuda (2021), Vertical eddy diffusivity in the subsurface pycnocline across the Pacific, *Journal of Oceanography*, *77*(2), 185-197, doi:10.1007/s10872-020-00589-9.

Karl, D., A. Michaels, B. Bergman, D. Capone, E. Carpenter, R. Letelier, F. Lipschultz, H. Paerl, D. Sigman, and L. J. Stal (2002), Dinitrogen fixation in the world's oceans, *Biogeochemistry*, *57/58*, 47-98.

Letelier, R. M., K. M. Bjorkman, M. J. Church, D. S. Hamilton, N. M. Mahowald, R. A. Scanza, N. Schneider, A. E. White, and D. M. Karl (2019), Climate-driven oscillation of phosphorus and iron limitation in the North Pacific Subtropical Gyre, *Proceedings of the National Academy of Sciences of the United States of America*, *116*(26), 12720-12728, doi:10.1073/pnas.1900789116.

Liang, Z., R. T. Letscher, and A. N. Knapp (2022), Dissolved organic phosphorus concentrations in the surface ocean controlled by both phosphate and iron stress, *Nature Geoscience*, *15*(8), 651-657, doi:10.1038/s41561-022-00988-1.

Luo, Y. W., I. D. Lima, D. M. Karl, C. A. Deutsch, and S. C. Doney (2014), Data-based assessment of environmental controls on global marine nitrogen fixation, *Biogeosciences*, *11*(3), 691-708, doi:10.5194/bg-11-691-2014.

Mahowald, N. M., A. R. Baker, G. Bergametti, N. Brooks, R. A. Duce, T. D. Jickells, N. Kubilay, J. M. Prospero, and I. Tegen (2005), Atmospheric global dust cycle and iron inputs to the ocean, *Global Biogeochemical Cycles*, *19*(4), n/a-n/a, doi:10.1029/2004gb002402.

Martiny, A.C., M. W. Lomas, W. Fu1, P. W. Boyd, Y. L. Chen, G. A. Cutter, M. J. Ellwood, K. Furuya, F. Hashihama, J. Kanda, D. M. Karl, T. Kodama, Q. P. Li, J. Ma, T. Moutin, E. M. S. Woodward, and J. K. Moore (2019), Biogeochemical controls of surface ocean phosphate. *Science Advances*, 5 (8), eaax0341, doi: 10.1126/sciadv.aax0341.

Mohr, W., T. Grosskopf, D. W. Wallace, and J. LaRoche (2010), Methodological underestimation of oceanic nitrogen fixation rates, *PLoS One*, *5*(9), e12583, doi:10.1371/journal.pone.0012583.

Moisander, P. H., R. A. Beinart, I. Hewson, A. E. White, K. S. Johnson, C. A. Carlson, J. P. Montoya, and J. P. Zehr (2010), Unicellular cyanobacterial distributions broaden the oceanic N_2 fixation domain, *Science*, *327*(5972), 1512-1514, doi:10.1126/science.1185468.

Monteiro, F. M., S. Dutkiewicz, and M. J. Follows (2011), Biogeographical

controls on the marine nitrogen fixers, *Global Biogeochemical Cycles*, *25*(2), n/a-n/a, doi:10.1029/2010gb003902.

Montoya, J. P., C. M. Holl, J. P. Zehr, A. Hansen, T. A. Villareal, and D. G. Capone (2004), High rates of N2 fixation by unicellular diazotrophs in the oligotrophic Pacific Ocean, *Nature*, *430*(7003), 1027-1031, doi:10.1038/nature02824.

Montoya, J. P., M. Voss, P. Kahler, and D. G. Capone (1996), A simple, high-precision, high-sensitivity tracer assay for N_2 fixation, *Applied and Environmental Microbiology*, *62*(3), 986-993.

Moore, M. C., et al. (2009), Large-scale distribution of Atlantic nitrogen fixation controlled by iron availability, *Nature Geoscience*, *2*(12), 867-871, doi:10.1038/ngeo667.

Obata, H., and C. M. G. van den Berg (2001), Determination of picomolar levels of iron in seawater using catalytic cathodic stripping voltammetry, *Analytical Chemistry*, *73*(11), 2522-2528, doi:10.1021/ac001495d.

Rouco, M., K. R. Frischkorn, S. T. Haley, H. Alexander, and S. T. Dyhrman (2018), Transcriptional patterns identify resource controls on the diazotroph *Trichodesmium* in the Atlantic and Pacific oceans, *ISME J*, *12*(6), 1486-1495, doi:10.1038/s41396-018-0087-z.

Sallée, J. B., V. Pellichero, C. Akhoudas, E. Pauthenet, L. Vignes, S. Schmidtko, A. N. Garabato, P. Sutherland, and M. Kuusela (2021), Summertime increases in upper-ocean stratification and mixed-layer depth, Nature, 591(7851), 592-598, doi:10.1038/s41586-021-03303-x.

Shiozaki, T., D. Bombar, L. Riemann, F. Hashihama, S. Takeda, T. Yamaguchi, M. Ehama, K. Hamasaki, and K. Furuya (2017), Basin scale variability of active diazotrophs and nitrogen fixation in the North Pacific, from the tropics to the subarctic Bering Sea, *Global Biogeochemical Cycles*, *31*(6), 996-1009, doi:10.1002/2017gb005681.

Shiozaki, T., Y. L. L. Chen, Y. H. Lin, Y. Taniuchi, D. S. Sheu, K. Furuya, and H.-Y. Chen (2014a), Seasonal variations of unicellular diazotroph groups A and B, and *Trichodesmium* in the northern South China Sea and neighboring upstream Kuroshio Current, *Continental Shelf Research*, *80*, 20-31, doi:10.1016/j.csr.2014.02.015.

Shiozaki, T., A. Fujiwara, M. Ijichi, N. Harada, S. Nishino, S. Nishi, T. Nagata, and K. Hamasaki (2018), Diazotroph community structure and the role of nitrogen fixation in the nitrogen cycle in the Chukchi Sea (western Arctic Ocean), *Limnology and Oceanography*, *63*(5), 2191-2205, doi:10.1002/lno.10933.

Shiozaki, T., K. Furuya, T. Kodama, S. Kitajima, S. Takeda, T. Takemura, and J. Kanda (2010), New estimation of N_2 fixation in the western and central Pacific Ocean and its marginal seas, *Global Biogeochemical Cycles*, *24*(1), n/a-n/a, doi:10.1029/2009gb003620.

Shiozaki, T., K. Furuya, T. Kodama, and S. Takeda (2009), Contribution of N_2 fixation to new production in the western North Pacific Ocean along 155°E, *Marine Ecology Progress Series*, *377*, 19-32, doi:10.3354/meps07837.

Shiozaki, T., M. Ijichi, T. Kodama, S. Takeda, and K. Furuya (2014b), Heterotrophic bacteria as major nitrogen fixers in the euphotic zone of the Indian Ocean, *Global Biogeochemical Cycles*, *28*(10), 1096-1110, doi:10.1002/2014gb004886.

Shiozaki, T., T. Kodama, and K. Furuya (2014c), Large-scale impact of the island mass effect through nitrogen fixation in the western South Pacific Ocean, *Geophysical Research Letters*, *41*(8), 2907-2913, doi:10.1002/2014gl059835.

Sohm, J. A., E. A. Webb, and D. G. Capone (2011), Emerging patterns of marine nitrogen fixation, *Nature Reviews Microbiology*, *9*(7), 499-508, doi:10.1038/nrmicro2594.

Suzuki, R., and T. Ishimaru (1990), An improved method for the determination of phytoplankton chlorophyll using N, N-dimethylformamide, *Journal of the Oceanographical Society of Japan*, *46*, 190-194.

Takemura, T. (2005), Simulation of climate response to aerosol direct and indirect effects with aerosol transport-radiation model, *Journal of Geophysical Research*, *110*(D2), doi:10.1029/2004jd005029.

Takemura, T., H. Okamoto, Y. Maruyama, A. Numaguti, A. Higurashi, and T. Nakajima (2000), Global three-dimensional simulation of aerosol optical thickness distribution of various origins, *Journal of Geophysical Research: Atmospheres*, *105*(D14), 17853-17873, doi:10.1029/2000jd900265.

Takemura, T., I. Uno, T. Nakajima, A. Higurashi, and I. Sano (2002), Modeling study of long-range transport of Asian dust and anthropogenic aerosols from East Asia, *Geophysical Research Letters*, *29*(24), 11-11-11-14, doi:10.1029/2002gl016251.

Tang, W., and N. Cassar (2019), Data-driven modeling of the distribution of diazotrophs in the global ocean, *Geophysical Research Letters*, 12258-12269, doi:10.1029/2019GL084376.

Tang, W., S. Wang, D. Fonseca-Batista, F. Dehairs, S. Gifford, A. G. Gonzalez, M. Gallinari, H. Planquette, G. Sarthou, and N. Cassar (2019), Revisiting the distribution of oceanic N_2 fixation and estimating diazotrophic contribution to marine production, *Nature Communication*, *10*(1), 831, doi:10.1038/s41467-019-08640-0.

Tanita, I., T. Shiozaki, T. Kodama, F. Hashihama, M. Sato, K. Takahashi, and K. Furuya (2021), Regionally variable responses of nitrogen fixation to iron and phosphorus enrichment in the Pacific Ocean, *Journal of Geophysical Research: Biogeosciences*, *126*(9), doi:10.1029/2021jg006542.

Wang, W. L., J. K. Moore, A. C. Martiny, and F. W. Primeau (2019),

Convergent estimates of marine nitrogen fixation, *Nature*, *566*(7743), 205-211, doi:10.1038/s41586-019-0911-2.

Ward, B. A., S. Dutkiewicz, C. M. Moore, and M. J. Follows (2013), Iron, phosphorus, and nitrogen supply ratios define the biogeography of nitrogen fixation, *Limnology and Oceanography*, *58*(6), 2059-2075, doi:10.4319/lo.2013.58.6.2059.

Watkins-Brandt, K. S., R. M. Letelier, Y. H. Spitz, M. J. Church, D. Böttjer, and A. E. White (2011), Addition of inorganic or organic phosphorus enhances nitrogen and carbon fixation in the oligotrophic North Pacific, *Marine Ecology Progress Series*, *432*, 17-29, doi:10.3354/meps09147.

Welschmeyer, N. A. (1994), Fluorometric analysis of chlorophyll *a* in the presence of chlorophyll *b* and phopigments, *Limnology and Oceanography*, *39*(8), 1985-1992.

Wen, Z., et al. (2022), Nutrient regulation of biological nitrogen fixation across the tropical western North Pacific, *Science Advances*, *8*(5), eabl7564, doi:10.1126/sciadv.abl7564.

Wilson, C., T. A. Villareal, N. Maximenko, S. J. Bograd, J. P. Montoya, and C. A. Schoenbaechler (2008), Biological and physical forcings of late summer chlorophyll blooms at 30°N in the oligotrophic Pacific, *Journal of Marine Systems*, *69*(3-4), 164-176, doi:10.1016/j.jmarsys.2005.09.018.

Yamaguchi, T., M. Sato, F. Hashihama, M. Ehama, T. Shiozaki, K. Takahashi, and K. Furuya (2019), Basin-scale variations in labile dissolved phosphoric monoesters and diesters in the central North Pacific Ocean, *Journal of Geophysical Research: Oceans*, *124*(5), 3058-3072, doi:10.1029/2018jc014763.

Yamaguchi, T., M. Sato, F. Hashihama, H. Kato, T. Sugiyama, H. Ogawa, K. Takahashi, and K. Furuya (2021), Longitudinal and vertical variations of dissolved labile phosphoric monoesters and diesters in the subtropical North Pacific, *Frontiers in Microbiology*, *11*, 570081, doi:10.3389/fmicb.2020.570081.

Zaheer, R., R. Morton, M. Proudfoot, A. Yakunin, and T. M. Finan (2009), Genetic and biochemical properties of an alkaline phosphatase PhoX family protein found in many bacteria, *Environmental Microbiology*, *11*(6), 1572-1587, doi:10.1111/j.1462-2920.2009.01885.x.

Zhu, A., V. Ramanathan, F. Li, and D. Kim (2007), Dust plumes over the Pacific, Indian, and Atlantic oceans: Climatology and radiative impact, *Journal of Geophysical Research*, *112*(D16), doi:10.1029/2007jd008427.